Journal of Engineering Technology and Applied Physics

LoRa Based IoT Enabled Sensor Networks for Plantations

Muhammad Luthfi Lokman[1, 2], Kah Yoong Chan[1, *], Yik Tian Ting[1], Chu Liang Lee[1], Gwo Chin Chung[3] and Wai Leong Pang[4]

[1]*Centre for Advanced Devices and Systems, Faculty of Engineering, Multimedia University, Persiaran Multimedia, 63100 Cyberjaya, Selangor, Malaysia.*
[2]*Intel Corporation, 11900 Bayan Lepas, Pulau Pinang, Malaysia.*
[3]*Centre for Wireless Technology, Faculty of Engineering, Multimedia University, Persiaran Multimedia, 63100 Cyberjaya, Selangor, Malaysia.*
[4]*School of Engineering, Taylor's University Lakeside Campus, 47500 Subang Jaya, Selangor, Malaysia.*
**Corresponding author*: kychan@mmu.edu.my, *ORCiD*: 0000-0003-1076-5034
https://doi.org/10.33093/jetap.2024.6.1.3
Manuscript Received: 29 July 2023, Accepted: 25 August 2023, Published: 15 March 2024

***Abstract* — The integration of Wireless Sensor Network (WSN) technology with the Internet of Things (IoT) in agriculture plays a pivotal role in addressing a range of challenges and constraints faced by the sector, encompassing issues such as labour shortages, suboptimal farm management practises, and unpredictable weather conditions. In response to these pressing concerns, this study focuses on the development of WSN with IoT for agriculture, employing a spread spectrum modulation technique named the Long Range (LoRa) module. By leveraging LoRa devices and wireless radio frequencies, this technology serves as a versatile platform for delivering wireless, long-range, and energy-efficient communication to support small and medium-sized agricultural operations. These operations often lack adequate technological assistance due to factors such as limited expertise and the high costs associated with cutting-edge agricultural technology. The research undertakes a comprehensive exploration, involving LoRa parameter testing, Line-of-Sight evaluations, Non-Line-Of-Sight (NLOS) simulations, and sensor calibration, to assess the efficacy of LoRa-based IoT-enabled sensor networks within plantation environments. The overarching objective of this research endeavour is to provide valuable insights that contribute to the optimisation of agricultural practises through streamlined IoT solutions. By implementing practical and cost-effective strategies, the local agricultural sector stands poised to achieve seamless strides in both sustainable and efficient food production.**

Keywords— Agriculture, WSN, IoT, LoRa, Sensor networks, Sustainable food production

I. INTRODUCTION

The Internet of Things (IoT) is distinguished by an intricate web of interconnected objects and devices that users can remotely control via the Internet, thereby providing elevated levels of convenience, comfort, efficiency, and security [1]. Capitalising on the pervasive accessibility of the Internet through a multitude of intelligent electronic devices, the evolution of the IoT has experienced swift proliferation, permeating various sectors including industry, retail, surveillance, agriculture, healthcare, and even domains as specific as poultry farming [1].

Emerging as one of the globe's largest palm oil producers and exporters [2], Malaysia's palm oil industry assumes a profoundly significant role within the nation's economic landscape [3]. In the broader context, agriculture holds a pivotal position, propelling numerous nations to amplify investments in these sectors to satisfy the unceasing demand for sustenance in the face of an escalating global populace. Predictions indicate an imminent 33 percent surge in the world's population, approaching nearly 10 billion in 2050, an increase from 7.6 billion as of October 2017. With projections envisioning a potential climb to 11.2 billion by 2100 [4], this trajectory unequivocally amplifies the need for nourishment, underscoring the requirement for a substantial 50 percent uptick in food production by 2050, even under modest economic expansion circumstances [4]. As this demographic pressure mounts, it is imperative for the agricultural sector to embark on further developmental strides and adopt novel technologies. To this end, a pragmatic

Published by MMU PRESS. URL: https://journals.mmupress.com/index.php/jetap/index

endeavour involves the deployment of real-time monitoring applications employing sensors, thus facilitating seamless oversight of plantation areas with statistical data accessible via a gamut of electronic devices such as smartphones, laptops, and tablets. Empowered by the advancements of the IoT, this innovative approach empowers both agricultural workers and farmers to promptly respond and enact preemptive measures to address emerging challenges.

The agricultural sector has traversed distinct phases of transformation, encompassing the First, Second, Third, and Fourth Revolutions [5]. These evolutionary milestones have ushered in notable enhancements, spanning modernised soil management practises, the advent of combustion engines powering mechanised farming implements, breakthroughs in genetic modifications, and culminating in the contemporary digital revolution. At present, the agricultural landscape, particularly within the plantation system, is on the cusp of a transformative fourth industrial revolution propelled by digitalization technologies. This paradigm shift is vividly exemplified through the convergence of agriculture with the Internet of Things (IoT), wherein traditional farming assumes a modern façade characterised by sensor-generated data transmitted seamlessly via wireless networks. This paradigm offers a substantial advantage by facilitating the wireless collection of data from agricultural sensors that are seamlessly connected to the internet, thus ushering in a new era of agricultural efficiency and innovation.

Long-range (LoRa) wireless communications have emerged as a transformative solution, propelling the modern agrotechnology sector towards optimised development in tandem with contemporary advancements. This technology catalyses an enhancement in both the quality and quantity of agricultural output by seamlessly integrating data informatics and communication technologies with progressive farming methodologies. This harmonisation encompasses a synergy between actuators, machinery, sensors, and the seamless connectivity facilitated by a Wireless Sensor Network (WSN) within the agricultural domain [6]. This heralds a convergence of diverse technologies under the umbrella of smart agriculture, utilising the prowess of the Internet of Things (IoT) to synergize with a global array of wireless sensors, robotics, precision soil mapping techniques, predictive decision-making systems, and more [7].

II. RELATED WORKS

Jeyashree and colleagues [8] devised an intelligent agricultural system utilizing LoRa Technology to enhance resource efficiency in farming. Their approach focused on real-time monitoring through long-range radio communication, facilitated by an Internet of Things (IoT) framework utilizing wireless sensor networks. The core hardware, named LSN50, operated as an outdoor gateway, ensuring ultra-long-range communication with minimal power consumption. Multiple transmitter nodes with various sensors communicated with the LSN50, which acted as a cloud-connected gateway. This setup enabled data collection and transmission, while the receiving gateway controlled actuators for an automatic sprinkler system, adjusting moisture levels in crop fields.

In the work by Gutiérrez and co-authors [9], another implementation of smart mobile LoRa Agriculture was presented, based on an IoT platform for agricultural monitoring. The system featured three key components: a mobile LoRaWAN gateway, sensor nodes, and a network server. A Raspberry Pi 3 B+ served as the primary gateway, supplemented by Heltec's HT-M01 as a sub-LoRa gateway. The sensor node, utilizing Heltec's 32 WiFi LoRa and DHT11 sensor, measured temperature and humidity levels in crop fields. The collected data was transmitted via The Thing Network (TTN) server and accessible through web applications or smartphones.

Reference [10] introduced a smart farming model utilizing LoRa technology and IoT devices. The Heltec ESP32 LoRa module processed signals and data through the SX1276 LoRa module. This system comprised two smart devices interconnected via LoRa, each equipped with DHT11 sensors and soil moisture sensors. Sensing data from the transmitter node was sent to the receiver node and stored in the cloud using the MQTT system.

Furthermore, in another LoRa application for agriculture outlined in reference [11], a comprehensive monitoring system for a starfruit plantation was established. The design featured Client and Master Nodes, each equipped with sensors and LoRa modules. Client nodes collected and processed sensor data, transmitting it via LoRa to the master node (receiver). Employing IoT-enabled sensors, this system facilitated real-time monitoring, while the user interface provided status updates accessible via desktops and smartphones. The user interface was responsive and adaptable, enabling prompt actions in response to command instructions. This innovative approach equips farmers with real-time monitoring capabilities, aiding in the informed execution of crop growth strategies.

III. PROPOSED SYSTEM

The system here encompasses three key components: the sensing module, the IoT platform, and mobile applications. The devised system employs an economical, single-channel gateway featuring a LoRa receiver node using ESP32 microcontroller and an LoRa transmitter node using Arduino Uno microcontroller. Figure 1 illustrates the overall block diagram of the proposed system.

Comprising a single microcontroller, the sensing modules are divided into distinct transmitter and receiver nodes. The transmitter node serves as the locus for crop condition measurements, wherein the embedded microcontroller functions as the operational center, executing commands in conjunction with various equipped sensing modules. These encompass the soil moisture sensor, environmental humidity and temperature sensor, light sensor, nutrient sensor, and LoRa module. Table I below shows the main function for all sensors which can implemented in this system.

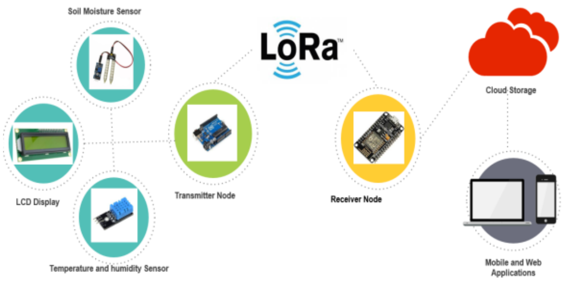

Fig. 1. Building block of system.

Table I: Main function for all sensor systems.

Sensor	Function
Temperature and humidity sensor	Monitors and regulates environmental conditions to optimize plant growth and prevent disease.
Soil Moisture Sensor	Measures soil moisture levels to ensure proper irrigation and prevent overwatering.
Light Sensor	Monitors light intensity for precise control of plant growth stages and energy-efficient cultivation.
Nutrient sensor	Analyses soil nutrient content to tailor fertilizer application and enhance crop health and yield.

The transmitter node for outdoor use is powered by a solar panel power module. Figure 2 and Fig. 3 show the LoRa Transmitter node circuit layout and its solar panel power module connections.

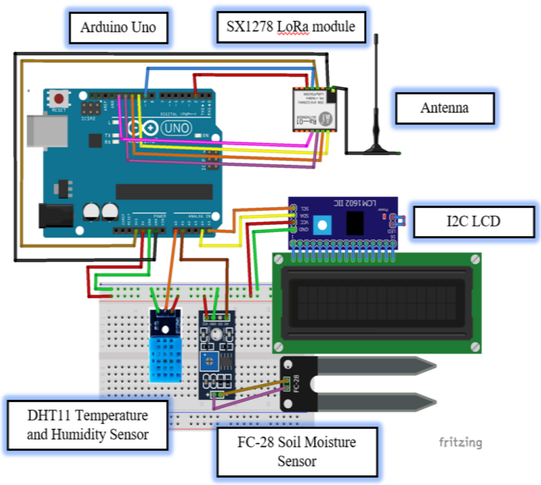

Fig. 2. LoRa transmitter node circuit layout.

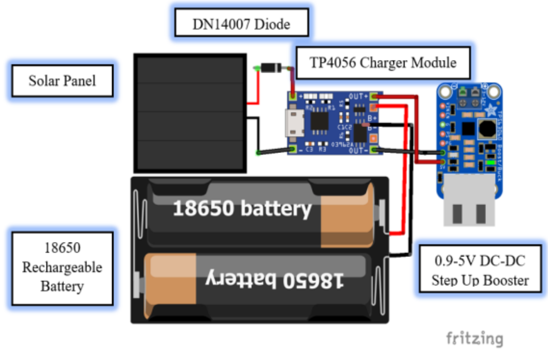

Fig. 3. Solar panel connection.

The receiver node serves as a gateway that facilitates smooth communication among the transmitter node, cloud database, and mobile application within the system architecture. Outfitted with internet-enabled microcontrollers and LoRa modules, this node receives sensory measurements from the transmitter node and subsequently transmits them wirelessly through the LoRa communication network to reach the receiver node. Once the data reaches the receiver node, it is read and forwarded to the cloud platform, where an IoT framework is integrated to store and aggregate the data for subsequent analysis. The schematic depiction of the LoRa Receiver Node's connections is presented in Fig. 4.

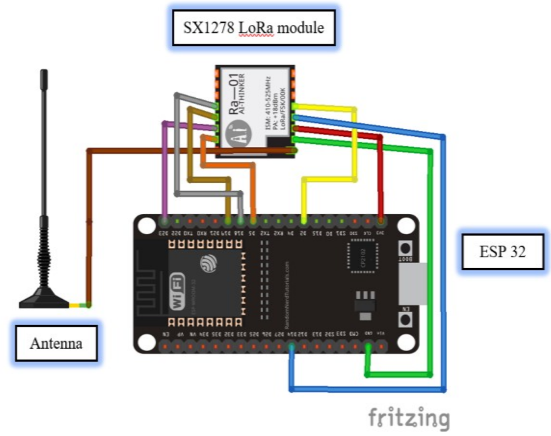

Fig. 4. LoRa receiver node.

Leveraging the power of the Internet network, transmitted data gains recognition and undergoes processing. Mobile technology assumes a pivotal role in this process, capturing and further processing the data within the cloud infrastructure and subsequently rendering the information visible through mobile devices. Notably, mobile applications like the Blynk app function as a comprehensive monitoring system, affording users the ability to exercise control from any location and at any time. These mobile applications establish a remote gateway, granting instant access to crucial information concerning the crop field's status. By harnessing the potential of IoT technology, this ecosystem facilitates the seamless collection, exchange, and processing of pertinent data related to the plantation, effectively mitigating the challenges encountered by farmers in the field. This interconnected framework empowers agricultural labourers and farmers to anticipate challenges and make informed decisions pre-emptively, effectively addressing potential issues on their plantations or farms.

IV. PROJECT DESIGN AND PACKAGING

The packaging contains two stages; transmitter and receiver nodes. For the transmitter node, the packing was developed using DIY material that is composed of polyvinyl chloride (PVC) pipe, while for the receiver node, the packing is built using 3D printing.

A. Transmitter Node D.I.Y. Packaging

The transmitter node was built from PVC plastic. The packing was designed to cater for the DHT11 temperature and humidity sensor and an antenna for the LoRa module. The FC-28 soil moisture sensors were placed on the bottom of the PVC cylinder, which was inserted and buried into the ground, as shown in Fig. 5.

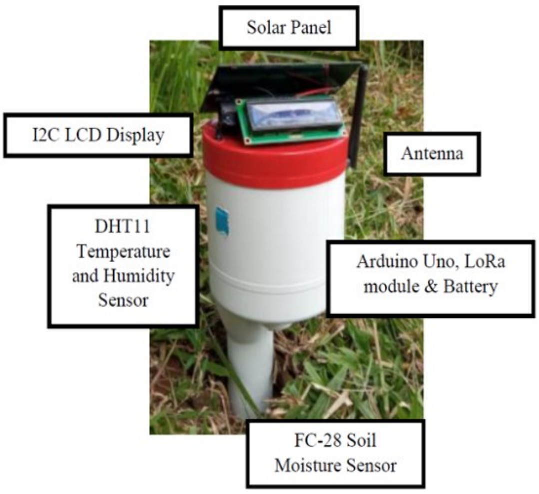

Fig. 5. Final prototype of transmitter node.

B. Receiver Node 3D Printing Packaging

The receiver node's casing was meticulously crafted using 3D printing technology, known as additive manufacturing. This innovative approach involves the layer-by-layer creation of a three-dimensional object using a computer-generated design. Advances in 3D packaging technology have democratised access, making it increasingly attainable to a wider audience; even individuals without specialised training can now conceive of 3D printing designs. This accessibility is attributed to the diminishing costs of owning a 3D printer and the availability of budget-friendly filament materials. The design process utilised the online tool TinkerCAD, renowned for its user-friendly interface and web-based accessibility, bypassing the need for local software installations. Employing basic techniques such as grouping, ungrouping, solidifying, and hollowing, the design was refined to precision. TinkerCAD's automatic alignment feature ensured optimal placement of components. Figure 6 showcases the 3D design of the LoRa Receiver Node case via TinkerCAD software, while Fig. 7 portrays the ultimate prototype of the LoRa Receiver Node case, exemplifying the culmination of this innovative process.

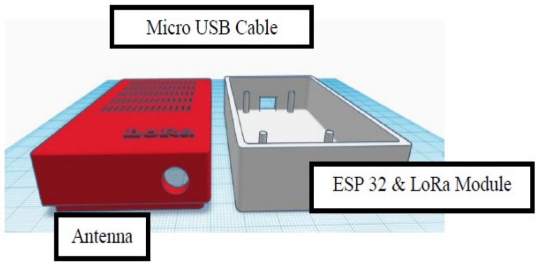

Fig. 6. 3D design of receiver node casing.

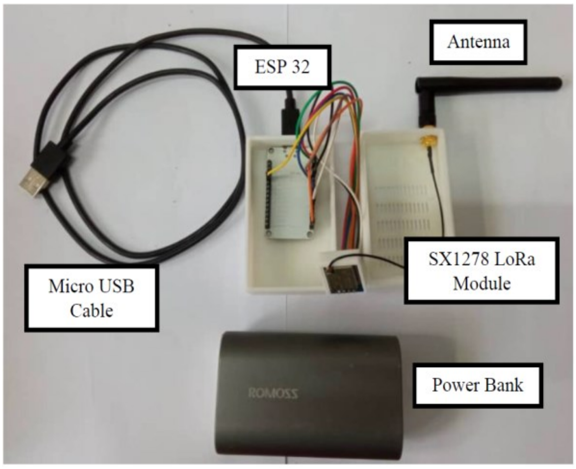

Fig. 7. Final prototype of receiver node.

V. THINGSPEAK IOT PLATFORM

Among the array of IoT platform services, Thingspeak stands out for its extensive usage, offering a robust framework for visualising and analysing live data streams alongside cloud storage capabilities. As wireless technology marches forward, IoT platforms are poised to assume a central role in facilitating the assimilation of cutting-edge technological advancements and innovations. Within this developmental context, an IoT device leveraging LoRa technology was engineered to furnish a comprehensive monitoring system for a crop field. The system's operational flow commences at the transmitter end, where sensory data is captured and transmitted to the receiver node, intricately linked to ThingSpeak. Within the receiver node, the pivotal ESP32 embodies the core IoT principles, forging a connection with the ThingSpeak platform. It adeptly gathers, records, and stores the sensory data, as well as the RSSI (Received Signal Strength Indicator) and SNR (Signal-to-Noise Ratio) values received through the cloud for subsequent processing. The amassed data is subsequently translated into meaningful insights and elegantly depicted in a graphical representation, as demonstrated in Fig. 8 below.

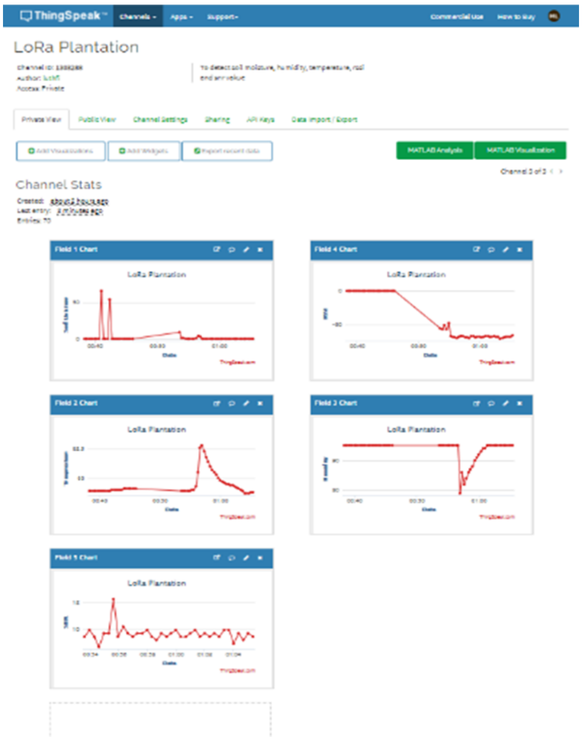

Fig. 8. ThingSpeak graphical chart.

VI. BLYNK MOBILE APPLICATION

Fig. 9. Blynk apps interface.

An Android smartphone was employed to show the sensor reading by using the mobile Blynk apps platform shown in Fig. 9. The Blynk app contains three major components, which are

- Blynk App - To create amazing interfaces and organise any projects using various widget functions and applications.

- Blynk Server – To provide communications between the smartphone and the hardware implementation. It is an open-source platform that allows users to use the Blynk Cloud or run it on a private Blynk server.

- Blynk Libraries –To enable communication between the server and the hardware interface by using incoming and outgoing commands through a specific code function.

Leveraging the Blynk app, remote access and monitoring of the sensor parameters housed within the transmitter node were seamlessly accomplished through smartphones. The app serves as an interface for visualising and displaying sensor data, facilitating both real-time observations and cloud-based storage. To harness the functionality of the Blynk app, an active Internet network connection is requisite. This entails linking the smartphone to a Wi-Fi network or utilising the mobile data plan for seamless access.

VII. LORA FIELD TEST AND PERFOMANCE

A. Line-Of-Sight (LOS)

Conducted within the suburban locale of Durian Tunggal, Melaka, the outdoor Line-of-Sight (LOS) test scrutinised the maximal transmission range. The evaluation encompassed distances ranging from 20 metres to a substantial 1000 metres. The assessment involved positioning the receiver in a fixed location while systematically relocating and measuring the transmitter at varying distances. Throughout this process, RSSI and SNR values were meticulously recorded across multiple distances, with an average computed from a series of five sequential transmissions to facilitate thorough data analysis. The receiver node, serving as the gateway module, was strategically stationed in Taman Nuri, Durian Tunggal, Melaka, possessing a specific latitude and longitude of 2.3217574186277843 and 102.27713894974104, respectively. The LoRa communication range between transmitter and receiver initiated at 20 metres and extended to 100 metres, as depicted in Fig. 10. In subsequent iterations, each progressive range extension incremented the distance between the transmitter and receiver by 200 metres, systematically expanding the assessment scope.

For both hardware and software components, uniform parameters were established for the LoRa module configuration of both the transmitter and receiver, ensuring consistent outdoor coverage. The specific device setup parameters are presented in Table II for reference.

Fig. 10. LOS google map view.

Table II: LOS LoRa parameter setup.

Parameter	Value
Transmit Power (dBm)	20
Spreading Factor	12
Bandwidth (kHz)	250
Code Rate	4/5
Antenna Gain (dBi)	3

Throughout the experimental tests, careful observation and recording of RSSI and SNR values were conducted for each range test. In instances where data corruption or the absence of a signal in LoRa communication occurred, the serial monitor ceased packet transmission, resulting in no available data for display. Consequently, the furthest distance achieved by the tested transmitter node became the upper limit of LoRa communication range. The recorded RSSI and SNR values spanning various ranges were subsequently averaged over a total of five interval transmissions and are presented in Table III for reference.

Table III: RSSI and SNR reading for LOS test.

Distance (m)	RSSI (dBm)	SNR (dB)
20	-105	6.00
40	-107	4.25
60	-111	0.50
80	-112	-4.25
100	-113	-8.75
200	-114	-14.50
400	-115	-15.50
600	-115	-15.75
800	-114	-17.50
900	-114	-18.25
923	-114	-19.25

Based on the findings presented in Table III, the investigation revealed a maximum discernible distance of 923 metres for LoRa communication connecting the receiver and transmitter. This range featured a corresponding RSSI of -114 dBm and an SNR of -19.25 dB. Evidently, LoRa communication undergoes degradation as the separation between transmitter and receiver expands, with observable implications for signal quality and integrity. The results further illuminate that enlarging the transmitter-receiver distance leads to signal attenuation and distortion, with the possibility of the signal encountering obstruction or disconnection at the farthest extents. Notably, the SNR analysis indicates that signal communication descends below the noise floor when the transmitter-receiver distance surpasses 80 metres, manifesting as a negative SNR output. A negative SNR value signifies a substantial discrepancy between signal and noise power, a characteristic shared with communication technologies like CDMA and WCDMA, which are designed to operate effectively under such conditions. This scenario is emblematic of the Non-Line-Of-Sight (NLOS) paradigm.

B. Non-Line-Of-Sight (NLOS)

NLOS testing involves evaluating radio frequency communication paths obstructed by intervening mediums, preventing direct signal reception. These obstructions, often stemming from tall buildings, houses, trees, or densely wired high-voltage zones, can fully or partially block signal propagation between transmitter and receiver devices. In the context of this study, the NLOS test was executed within a residential setting situated in Taman Rajawali 4, Durian Tunggal, Melaka. The residential building blocks served as the designated obstacles for this experiment, as depicted in Fig. 11 below.

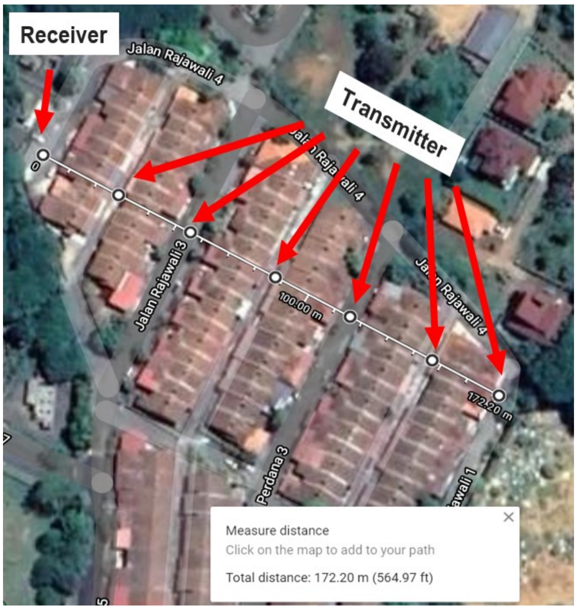

Fig. 11. NLOS google map view.

The experimentation was conducted within the residential confines of Taman Rajawali, Durian Tunggal, Melaka. In this setup, the transmitter was positioned amidst the interstitial space between building blocks, while the receiver remained fixed at specific coordinates, characterized by a latitude of

2.31892736293414 and a longitude of 102.2804814056584.

Leveraging LoRa's capacity to penetrate through multiple walls or structures, the signal bandwidth was meticulously configured at 125 kHz, coupled with a spreading factor of 12. The strategic combination of a low bandwidth and a high spreading factor culminates in extended distance coverage, consequently enhancing the wireless communication sensitivity of the devices. Notably, both the transmitter and receiver devices adhered to identical parameters, encompassing congruent settings for spreading factor, bandwidth, and coding rate. The parameter configuration for both transmitter and receiver units is presented in Table IV below for your reference.

Table IV: NLOS transmitter and receiver LoRa parameter.

Parameter	Value
Transmit Power (dBm)	20
Spreading Factor	12
Bandwidth (kHz)	125
Code Rate	4/5

In entirety, measurements were taken for LoRa communication RSSI and SNR values across a span of more than six blocks of terrace house obstacles. For each test case, five sets of data were captured at 10-second intervals and subsequently averaged to derive representative RSSI and SNR values. The resulting average values, pertaining to various quantities of building blocks, are presented in Table V below.

Table V: RSSI and SNR value for NLOS test.

No. of Buildings	Distance (m)	RSSI (dBm)	SNR (dB)
1	26.14	-92.8	1.8
2	55.97	-95.4	-14.05
3	86.37	-96.2	-15.85
4	114.71	-96.6	-17.95
5	146.86	-97.8	-29.3
6	172.20	NAN	NAN

Based on the outcomes documented in Table V, the average RSSI fluctuated within the range of -92 dBm to -98 dBm. Impressively, the signal successfully traversed an expanse encompassing five blocks of buildings, underscoring its potency. However, the Non-Line-Of-Sight (NLOS) examination, involving six distinct building scenarios, culminated in a failure of LoRa module communication. Regrettably, neither signal was successfully received by the designated receiver. This setback emanated from the positioning of the transmitter, which is situated in proximity to a neighbouring substation tower. The signal distortion caused the transmitter signal to be blocked from transmiting to the receiver side. Intriguingly, a deeper analysis, as demonstrated in Table III, highlights the noticeable contrast between line-of-sight (LOS) and NLOS tests. The signal strength in NLOS conditions showcased discernible weakness, with a maximum transmitter distance of 146.86 meters across five building blocks. The communication link abruptly terminated at the sixth building block, with a transmitter-receiver distance of 172.20 meters. These insights emphasize the pivotal role of obstacles in signal propagation, indicating that fewer obstructions yield superior LoRa coverage. Consequently, it is evident that unobstructed sightlines or locales characterized by diminished obstacles can greatly enhance the sensitivity and effectiveness of wireless LoRa communication.

C. *Effect of Different LoRa Parameter*

The outdoor testing phase unfolded within the suburban environs of Kampung Pulau, Durian Tunggal, Melaka. Five distinct measurement locations were meticulously selected, each positioned vertically in a linear alignment, with precise intervals of 10m, 20m, 30m, 40m, and 50m, as thoughtfully detailed in Table VI. Throughout the testing endeavours, the experimental setup featured a solitary transmitter node and a corresponding receiver node. While the receiver node was strategically situated indoors, boasting a latitude and longitude of 2.31517362401402 and 102.27820983143403, respectively, the LoRa transmitter node was methodically relocated across the designated locations for each testing iteration. The measurement of distances between transmitter and receiver nodes was executed using both a measuring tape and the Google Maps satellite measuring tools for approximate verification. Illustrated in Fig. 12 is the Google Maps satellite perspective, elucidating the layout of the five distinct locations earmarked for the varied LoRa parameter tests.

Fig. 12. Location of LoRa parameter test.

Table VI: Outdoor location for LoRa parameters test.

Location	Distance(m)
A	10
B	20
C	30
D	40
E	50

Table VII below summarizes the six testing modes of different LoRa parameters. The testing modes were carried out using spreading factors of 7, 9, and 12, and a bandwidth of 125 kHz and 250 kHz, respectively. The coding rate values for these testing modes were set to be 4/5.

Table VII: List for different LoRa parameters.

Mode	Spreading Factor	Bandwidth (kHz)	Coding Rate
1	7	125	4/5
2	7	250	
3	9	125	
4	9	250	
5	12	125	
6	12	250	

For every test location, the RSSI and SNR values were meticulously logged, encompassing various modes defined by distinct parameters such as spreading factor and bandwidth. Across five discrete datasets, measurements were taken at 10-time intervals, with the average value subsequently employed for subsequent analysis. To enhance the clarity of the results, all RSSI and SNR values within each mode were graphically represented. This visual representation facilitated a mode-by-mode comparison, allowing for the observation of differences in SNR and RSSI values, as depicted in Fig. 13 and Fig. 14, respectively.

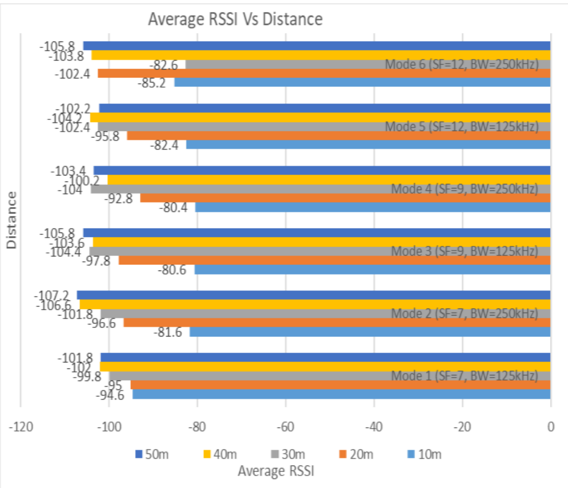

Fig. 13. Average RSSI (dBm) for each mode.

Within the realm of LoRa communication, RSSI stands as an abbreviation for Received Signal Strength Indication, measured in dBm and represented as a negative value. As delineated in Fig. 13 above, the collective average RSSI values across all modes spanned the interval of -82 dBm to -107 dBm. Notably, the graphical representation indicates that, on average, location A situated at a distance of 10 metres from the receiver exhibited the lowest RSSI value, while location E, positioned 50 metres away, yielded the highest RSSI value. The proximity of the RSSI value to 0 signifies heightened signal strength. Moreover, an elevation in spreading factor coupled with an identical bandwidth length induced a decrease in the average RSSI value, thereby augmenting signal stability and strength. This trend is evident in the juxtaposition of Mode 1, Mode 3, and Mode 5, each featuring distinct spreading factors (7, 9, and 12), while maintaining a constant bandwidth of 125 kHz. Similarly, employing the same spreading factor but varying the bandwidth contributes to fluctuations in the RSSI values. A lower bandwidth (125 kHz) correlates with a more favourable RSSI value in contrast to a higher bandwidth (250 kHz).

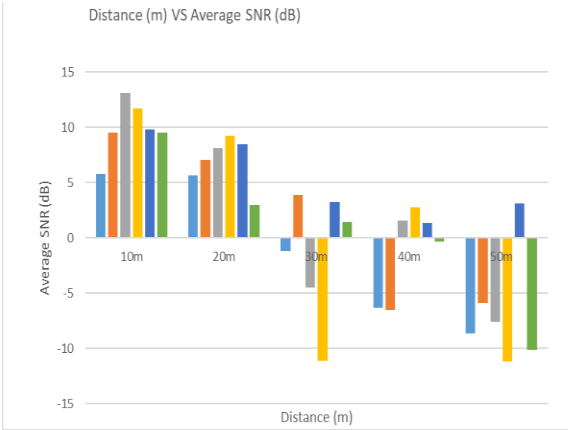

Fig. 14. Average SNR (dB) for each mode.

Illustrated in Fig. 14 above is the Signal-to-Noise Ratio (SNR) graph, a visual depiction encapsulating the relationship between the power of the received signal and the potentially disruptive background noise that may interfere with or obstruct signal transmission. Discerning from the graph, both locations D and E, situated at 40 meters and 50 meters from the receiver, respectively, manifest the highest levels of noise interference. In contrast, locations A, B, and C, positioned within the sub-30 meter range, exhibit diminished SNR values and thus a reduced noise interface. It's noteworthy that SNR values greater than '0 signify signal reception above the noise floor, whereas values less than '0 indicate signal reception beneath the noise floor. Conventionally, the LoRa SNR value resides within the scope of -20 dB to +10 dB.

Crucially, as the SNR value approaches +10 dB, the susceptibility of the received signal to corruption diminishes. Within this context, location A emerges as a standout, boasting the highest average SNR across all modes. Conversely, location E exhibits the lowest average SNR value among all modes, indicating heightened noise interference that potentially compromised signal integrity, distinguishing it from other locations. In tandem with the escalating spreading factor (7, 9, and 12) in concurrence with distance amplification, while retaining consistent bandwidths, an elevation in the SNR value incurs a reduction in SNR, save for Mode 4's spreading factor of 9. Additionally, augmenting the bandwidth length from 125 kHz to 250 kHz while maintaining a consistent spreading factor leads to an SNR value escalation along with intensified noise interference.

Noteworthy exceptions include spreading factor 7 within Modes 1 and 2.

VIII. CONCLUSION

In conclusion, the successful realization of a cost-effective, single-channel LoRa gateway and uncomplicated end devices—comprising the ESP32 microcontroller for the receiver node and the Arduino Uno microcontroller for the transmitter node—has propelled the advancement of IoT-empowered sensor technology, tailored for monitoring applications within plantations. The amassed data underscored the efficacy of the LoRa-driven WSN in overseeing plantations and farms. Prospects for augmenting the LoRa range lie in the manipulation of parameters such as spreading factor, bandwidth, and coding rate. Elevating the spreading factor can enhance LoRa transmission performance, while a narrower bandwidth configuration may extend the range of LoRa communication, bolstering its resilience against signal noise. The IoT landscape was founded on ThingSpeak and Blynk applications, both pivotal in data processing and functioning as cloud servers. The developed LoRa IoT WSN here demonstrates a low-cost solution for monitoring and management of plantations and farms, which is important in transforming these industries in the era of IR 4.0. Furthermore, the comprehensive exploration of diverse experiments encompassing LoRa parameter testing, Line-of-Sight, Non-Line-Of-Sight (NLOS) simulations, and sensor calibration provides valuable insights into the efficacy of LoRa-based IoT-enabled sensor networks within plantations. The findings derived from these experiments contribute to a deeper understanding of how such networks perform in real-world conditions, thus paving the way for the optimized implementation of LoRa technology in agricultural settings.

ACKNOWLEDGEMENT

This research is funded by the Internal Fund of Multimedia University, Cyberjaya Campus.

REFERENCES

[1] N. A. A. Hamzah, M. R. Abu Saad, W. Z. Wan Ismail, T. Bhunaeswari and N. Z. Abd Rahman, "Development of A Prototype of An IoT Based Smart Home with Security System Flutter Mobile," *J. Eng. Technol. Appl. Phys.*, vol. 1, no. 2, pp. 34–41, 2019.

[2] W. Li, H. Fu, L. Yu and A. Cracknell, "Deep Learning Based Oil Palm Tree Detection and Counting for High-Resolution Remote Sensing Images," *Remote Sens.*, vol. 9(1), No. 22, 2017.

[3] C. C. Lee, S. Y. Tan, T. S. Lim and V. C. Koo, "Oil Palm Tree Detection from High Resolution Drone Image Using Convolutional Neural Network," *J. Eng. Technol. Appl. Phys.*, vol. 1, no. 2, pp. 6–9, 2019.

[4] "*The Future of Food and Agriculture: Trends and Challenges*," Food and Agriculture Organization of the United Nations, Rome, Italy, 2017.

[5] M. Briers, "*Digital Farming and the 4th Agricultural Revolution*," Food Agility, 23 October 2018. https://www.foodagility.com/posts/digital-farming-and-the-4th-agricultural-revolution.

[6] D. Pivoto, P. D. Waquil, E. Talamini, C. P. S. Finocchio, V. F. Dalla Corte and G. de Vargas Mores, "Scientific Development of Smart Farming Technologies and Their Application in Brazil," *Inform. Process. Agricult.*, vol. 5, no. 1, pp. 21–32, 2018.

[7] O. Elijah, T. A. Rahman, I. Orikumhi, C. Y. Leow and M. N. Hindia, "An Overview of Internet of Things (IoT) and Data Analytics in Agriculture: Benefits and Challenges," *IEEE Internet of Things J.*, vol. 5, No. 5, pp. 3758-3773, 2018.

[8] P. Jeyashree, M. Meghana and B. S. Reddy, "Smart Agriculture Using Lora Technology," *Int. J. Emerg. Technol. Innov. Eng.*, vol. 5, no. 4, pp. 216-220, 2019.

[9] S. Gutiérrez, I. Martínez, J. Varona, M. Cardona and R. Espinosa, "Smart Mobile LoRa Agriculture System based on Internet of Things," in *IEEE 39th Central America and Panama Conven.*, Guatemala, pp. 1-6, 2019.

[10] R. K. Kodali, S. Yerroju and S. Sahu, "Smart Farm Monitoring Using LoRa Enabled IoT,," in *Second Int. Conf. Green Comput. and Internet of Things*, Bangalore, India, pp. 391-394, 2018.

[11] A. F. Rachmani and F. Y. Zulkifli, "Design of IoT Monitoring System Based on LoRa Technology for Starfruit Plantation," in *Proc. TENCON 2018 - 2018 IEEE Region 10 Conference*, Jeju, Korea, pp. 1241-1245, 2018.